3D modelling of Rayleigh wave acoustic emission from a crack under stress

W. Ben Khalifa, K. Jezzine, Sébastien Grondel

ACOUSTICS 2012

3D modelling of Rayleigh wave acoustic emission from a crack under stress

W. Ben Khalifa[a], K. Jezzine[a] and S. Grondel[b]

[a]CEA-LIST, Bâtiment 611 - Point Courrier 120, 91191 Gif-Sur-Yvette Cedex, France
[b]IEMN-DOAE, Université de Valenciennes et du Hainaut Cambrésis, Le Mont Houy, 59313 Valenciennes Cedex 9, France
warida.ben-khalifa@cea.fr

Acoustic emission (AE) is a non-destructive testing method used in many industrial applications (testing for leaks, or monitoring weld quality, etc…) for the examination of large structures subjected to various stresses (e.g. mechanical loading) in different domains (aerospace, pressure-vessel industries in general, etc...). The energy released by a defect under stress can propagate as guided waves in thin structures or as surface Rayleigh waves in thick ones. A limited number of sensors placed at various positions are needed to monitor large structure. Then, AE-data analysis is used to calculate the spatial location of the signal origin by using the signal arrival times at a number of sensors. The French Atomic Energy Commission is engaged in the development of a tool for simulating AE examinations. These tools are based on specific models for the AE sources, for the propagation of guided or Rayleigh waves and for the behavior of AE sensors. Here, the coupling of a fracture mechanics based model for AE source model and Green functions of Rayleigh wave is achieved through an integral formulation relying on the elastodynamic reciprocity principle. Predictions computed with this three dimensional model are compared to results from the literature for validation purpose.

1. Introduction

The far field acoustic emission from a crack under stress is dominated by the presence of Rayleigh wave. In fact, in a three dimensional geometry, surface wave decay as $r^{-1/2}$ and bulk waves decay as r^{-1}, where r is the distance between the source and an observation point.

Some methods have been developed in the literature to calculate the acoustic emission from a crack, using the reciprocity principle and based on different AE source models, hypothesis and approximations.

For instance, Harris and Pott [1] have developed a Rayleigh wave acoustic emission model from buried crack that predicts Rayleigh wave excited by the starting of a faulting event. The surface wave was expressed by an integral formulation relying on the elastodynamic reciprocity theorem. This formulation combines bulk waves emitted by the starting event and the Rayleigh wave components of the Green's tensor, calculated in [2] from the coupling between the P-wave and S-wave component (SV) polarized in the plane of incidence.

The Rayleigh wave displacement is then evaluated by the application of the stationary phase technique and the particle velocity of the emitted wave is approximated near the Rayleigh wave arrival time.

In this paper we present an acoustic emission formulation to predict the Rayleigh wave emitted by a propagation of a crack under stress in a three dimensional geometry. This method was presented by Achenbach [3] for a two dimensional acoustic emission problem. This model combines Rayleigh wave Green functions and the crack opening displacement obtained by the exact complex solution from fracture mechanics.

The Rayleigh wave Green functions are obtained from the application of the reciprocity principle in cylindrical coordinate system following the method presented by Achenbach in [4].

2. AE model

In three-dimensional geometry, the displacement of the Rayleigh wave emitted by the propagation of a crack under stress is calculated from the application of the reciprocity theorem; this theorem connects two different elastodynamic states, state A and state B.

In the frequency domain, the reciprocity principle for a body of volume V and surface S can be written as:

$$\int_V \left[f_i^A u_i^B - f_i^B u_i^A \right] dV = \int_S \left[\tau_{ij}^B u_i^A - \tau_{ij}^A u_i^B \right] n_j dS \,. \quad (1)$$

where n_i are the components of the outward normal to S, f_i , u_i and τ_{ij} are the components of body forces, displacements and stresses.

2.1. Application of the reciprocity theorem

We select state A as the solution of the acoustic emission problem and state B as the Rayleigh wave emitted by a point source applied in the x_k direction *(x_k=x_1, x_2 or z)*

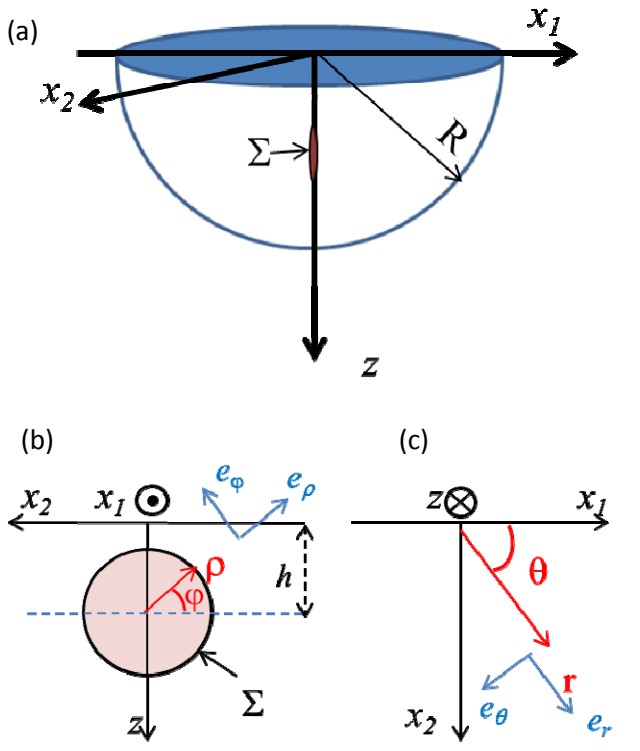

Figure 1: (a) geometry of the acoustic emission problem (b) geometry of the crack and definition of the local cylindrical coordinate system *(ρ, φ, x_1)* and (c) definition of the global cylindrical coordinate system *(r, θ, z)*

We apply the reciprocity equation to the region of the half space defined in Figure 1 where Σ is the surface of the crack located in the *(x_2,z)* plan.

The integral over the free surface and the hemisphere of radius R as $R \to \infty$ vanishes and the reciprocity equation can be written as:

$$u_k^A(\xi) = \int_\Sigma \left[u_{i,k}^G(X,\xi)\tau_{ij}^A - u_i^A \tau_{ij,k}^G(X,\xi) \right] n_j(X) d\Sigma(X) \quad (2)$$

Where $u_{i,k}^G$ and $\tau_{ij,k}^G$ are respectively the displacement and stress components of the Rayleigh Green's tensor.

$X=(r,\theta,z)$ and $\xi=(r_0,\theta_0,z_0)$ are respectively the positions of the observation point and the source.

2.2. Rayleigh wave components of the Green's function

We have calculated the displacement of Rayleigh wave generated by a point load in a cylindrical coordinate system by the application of the reciprocity theorem [4].

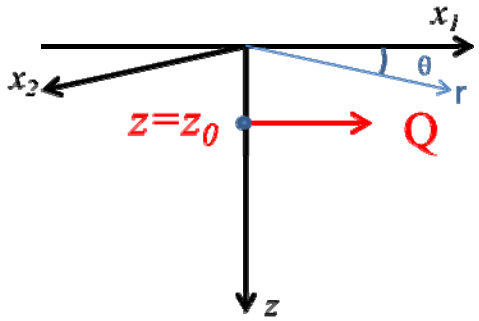

Figure 2: half space subjected to a point load at $z=z_0$.

The displacement components of Rayleigh wave generated by a point load of magnitude Q (Figure 2) applied at $z=z_0$ in the x_1 direction are:

$$u_{r,1} = \frac{k_R}{4i}\frac{QV^R(z_0)}{I}V^R(z)\Phi'(k_R r)cos\theta \quad (3)$$

$$u_{\theta,1} = \frac{k_R}{4i}\frac{QV^R(z_0)}{I}V^R(z)\left(\frac{-1}{rk_R}\right)\Phi(k_R r)sin\theta \quad (4)$$

$$u_{z,1} = \frac{k_R}{4i}\frac{QV^R(z_0)}{I}W^R(z)\Phi(k_R r)cos\theta \quad (5)$$

where $\Phi'(x) = \frac{d\Phi}{dx}$.

In the case of a point load of magnitude M in the x_2 direction we have:

$$u_{r,2} = -\frac{k_R}{4i}\frac{MV^R(z_0)}{I}V^R(z)\Phi'(k_R r)\sin\theta \quad (6)$$

$$u_{\theta,2} = \frac{k_R}{4i}\frac{MV^R(z_0)}{I}V^R(z)\left(\frac{-1}{rk_R}\right)\Phi(k_R r)\cos\theta \quad (7)$$

$$u_{z,2} = -\frac{k_R}{4i}\frac{MV^R(z_0)}{I}W^R(z)\Phi(k_R r)\sin\theta \quad (8)$$

In the case of a point load of magnitude P in the z direction we have:

$$u_{r,z} = -\frac{k_R}{4i}\frac{PW^R(z_0)}{I}V^R(z)\Phi_0'(k_R r) \quad (9)$$

$$u_{\theta,z} = 0 \quad (10)$$

$$u_{z,z} = -\frac{k_R}{4i}\frac{PW^R(z_0)}{I}W^R(z)\Phi_0(k_R r) \quad (11)$$

Where:

$$I = \int_0^\infty \left[T_{rr}^R(z)V^R(z) - T_{rz}^R(z)W^R(z) \right] dz \quad (12)$$

$$W^R(z) = d_3 e^{-pz} - e^{-qz} \quad (13)$$

$$V^R(z) = d_1 e^{-pz} + d_2 e^{-qz} \quad (14)$$

$$T_{rr}{}^R(z) = \mu\left[d_4 e^{-pz} + d_5\, e^{-qz} \right] \quad (15)$$

$$T_{rz}{}^R(z) = \mu\left[d_6\, e^{-pz} + d_7\, e^{-qz} \right] \quad (16)$$

d_1, d_2, d_3, d_4, d_5, d_6, and d_7 are defined by:

$$d_1 = -\frac{1}{2}\frac{k_R^2+q^2}{k_R p} \quad (17)$$

$$d_2 = \frac{q}{k_R} \quad (18)$$

$$d_3 = \frac{1}{2}\frac{k_R^2+q^2}{k_R} \quad (19)$$

$$d_4 = \frac{1}{2}(k_R^2+q^2)\frac{2p^2+k_R^2-q^2}{pk_R^2} \quad (20)$$

$$d_5 = -2q \quad (21)$$

$$d_6 = \frac{k_R^2+q^2}{k_R p} \quad (22)$$

$$d_7 = -\frac{k_R^2+q^2}{k_R p} \quad (23)$$

The quantities p and q are defined by:

$$p^2 = k_R^2 - k_l^2 \quad (24)$$

$$q^2 = k_R^2 - k_t^2 \quad (25)$$

and 37

$$\Phi\left(k_R r\right) = H_1^{(1)}(k_R r) \tag{26}$$

$$\Phi_0\left(k_R r\right) = H_0^{(1)}(k_R r) \tag{27}$$

$H_n^{(1)}$ is the first kind Hankel function of order n.
The compressional and shear wave numbers are:

$$k_l = \omega\left(\frac{\rho}{(\lambda+2\mu)}\right)^{\frac{1}{2}} \tag{28}$$

$$k_t = \omega\left(\frac{\rho}{\mu}\right)^{\frac{1}{2}} \tag{29}$$

The Rayleigh wave number is:

$$k_R = k_t \big/ \eta_R \tag{30}$$

Where

$$\eta_R = \frac{0.87+1.12\nu}{1+\nu} \tag{31}$$

ρ, ν, λ and μ are respectively the density of the medium, Poisson ratio and the elastic Lamé constants defined by: $\lambda = \frac{E\nu}{(1+\nu)(1-2\nu)}$ and $\mu = \frac{E}{2(1+\nu)}$, where E is the Young's modulus.

We express the Green tensor in the cylindrical coordinate using the superposition principle:

$$G^R = \begin{pmatrix} u_{r,r} & u_{r,\theta} & u_{r,z} \\ u_{\theta,r} & u_{\theta,\theta} & u_{\theta,z} \\ u_{z,r} & u_{z,\theta} & u_{z,z} \end{pmatrix} \tag{32}$$

where:

$$u_{r,r} = \frac{k_R}{4i}\frac{V^R(z_0)}{I}V^R(z)\Phi'\left(k_R r\right)\left((\cos\theta)^2 - (\sin\theta)^2\right) \tag{33}$$

$$u_{\theta,r} = \frac{k_R}{4i}\frac{V^R(z_0)}{I}V(z)\left(\frac{-1}{rk_R}\right)\Phi\left(k_R r\right)\left(2\cos\theta sin\theta\right) \tag{34}$$

$$u_{z,r} = \frac{k_R}{4i}\frac{V^R(z_0)}{I}W(z)\Phi\left(k_R r\right)\left((\cos\theta)^2 - (\sin\theta)^2\right) \tag{35}$$

$$u_{r,\theta} = \frac{k_R}{4i}\frac{V^R(z_0)}{I}V(z)\Phi'\left(k_R r\right)\left(-2\sin\theta cos\theta\right) \tag{36}$$

$$u_{\theta,\theta} = \frac{k_R}{4i}\frac{V^R(z_0)}{I}V(z)\left(\frac{-1}{rk_R}\right)\Phi\left(k_R r\right)\left(1-2(\sin\theta)^2\right) \tag{38}$$

$$u_{z,\theta} = \frac{k_R}{4i}\frac{V^R(z_0)}{I}W(z)\Phi\left(k_R r\right)\left(-2\sin\theta cos\theta\right) \tag{39}$$

2.3. Rayleigh wave acoustic emission

Eq. (2) can be written as:

$$u_k^A(\xi) = \int_{\Sigma^+}\left[u_{i,k}^G(X,\xi)\tau_{ij}^A - u_i^A\tau_{ij,k}^G(X,\xi)\right]n_j(X)d\Sigma^+(X) + \int_{\Sigma^-}\left[u_{i,k}^G(X,\xi)\tau_{ij}^A - u_i^A\tau_{ij,k}^G(X,\xi)\right]n_j(X)d\Sigma^-(X) \tag{40}$$

Σ^+ and Σ^- are respectively the crack surface on $x_1=0^+$ and $x_1=0^-$.

We assume that the crack is a surface of displacement discontinuity. In the case of a tensile stress (Mode I), the displacement at the surface of the crack in the global cylindrical coordinate system is:

$$u_\theta^A = u_1^A \tag{41}$$

Eq. (41) can be written as:

$$u_k^A(\xi) = \int_{\Sigma^+}\left[-\Delta u_\theta^A\tau_{\theta\theta,k}^G(X,\xi)\right]n_\theta(X)d\Sigma^+(X) \tag{42}$$

Where

$$\Delta u_\theta^A = u_\theta^A\big|_{x_1=0^+} - u_\theta^A\big|_{x_1=0^-} \tag{43}$$

The integral over the surface Σ^+ can be written as:

$$u_k^A(\xi) = \int_{\Sigma^+} -\Delta u_\theta^A\left(\lambda\frac{\partial u_{r,k}^G(X,\xi)}{\partial r} + (\lambda+2\mu)\frac{1}{r}\left(\frac{\partial u_{\theta,k}^G(X,\xi)}{\partial\theta} + u_{r,k}^G(X,\xi)\right) + \lambda\frac{\partial u_{z,k}^G(X,\xi)}{\partial z}\right)d\Sigma^+(X) \tag{44}$$

As $u_{i,k}^G(X,\xi) = u_{k,i}^G(\xi,X)$,

$$u_k^A(\xi)=\int_{\Sigma^+}-\Delta u_\theta^A\left(\lambda\frac{\partial u_{k,r}^G(\xi,X)}{\partial r}+(\lambda+2\mu)\frac{1}{r}\left(\frac{\partial u_{k,\theta}^G(\xi,X)}{\partial\theta}+u_{k,r}^G(\xi,X)\right)+\lambda\frac{\partial u_{k,z}^G(\xi,X)}{\partial z}\right)d\Sigma^+(X) \quad (45)$$

We simplify the expression by considering a dipole acting at $z=h$, as shown in figure (1), i.e. $X=(0, 0, h)$:

$$u_k^A(\xi)=\left(\lambda\frac{\partial u_{k,r}^G(\xi,h)}{\partial r}+(\lambda+2\mu)\frac{1}{r}\left(\frac{\partial u_{k,\theta}^G(\xi,h)}{\partial\theta}+u_{k,r}^G(\xi,h)\right)+\lambda\frac{\partial u_{k,z}^G(\xi,h)}{\partial z}\right)\int_0^a\int_0^{2\pi}-\Delta u_1^A\,\rho\,d\rho\,d\varphi \quad (46)$$

2.4. Acoustic emission source

In the case of tensile circular crack of radius a loaded by uniform pressure σ on its faces, the crack opening displacement (COD), expressed from the complex solution issued from fracture mechanics in the local cylindrical coordinate system (ρ, φ, x_1) can be looked up from a book on fracture mechanics:

$$\Delta u_1(\rho,t)=2\frac{4(1-\nu^2)\sigma}{\pi E}\sqrt{a(t)^2-\rho^2} \quad (47)$$

3. Simulation of AE

We assume that the crack diameter evolves from $l_0=1\text{mm}$ to $l=5\text{mm}$ at a velocity $V=2000\text{m/s}$ during $T=0.8\mu s$, we consider a sampling frequency $F_e=50\,MHz$ and $\sigma=200MPa$.

We define ρ_j and t_n as:

$$\rho_j=jV\Delta t \quad (48)$$

$$t_n=t_0+n\frac{1}{Fe} \quad (49)$$

j varies from 0 to $J/2$, and n varies from 0 to N where:

$$\Delta t=1/F_e \quad (50)$$

$$N=\frac{T}{\Delta t} \quad (51)$$

$$J=\frac{l}{V\Delta t} \quad (52)$$

Eq.(40) can be discretised as follows:

$$\Delta u_1(\rho_j,t_n)=2\sigma\frac{4(1-\nu^2)}{\pi E}\sqrt{((l_0+nV\Delta t)/2)^2-\rho_j^2} \quad (53)$$

for $r_j\le(l_0+nV\Delta t)/2$

$$\Delta u_1(r_j)=0 \quad (54)$$

for $(l_0+nV\Delta t)/2\le r_j\le l/2$

We take the Fourier transform of the COD Eq. (53) to obtain the displacement field of the emitted Rayleigh wave in the frequency domain given by Eq. (47).

The displacement field in the time domain is then obtained using the inverse Fourier Transform of Eq. (47).

We have simulated the velocity of the Rayleigh wave emitted from the propagation of a circular crack under stress, located at a distance z_0 from the surface; figure 3 presents the normalized velocity as a function of τ where

$$\tau=t\frac{v_R}{z_0}-\frac{r}{z_0}-T\frac{v_R}{z_0} \quad (55)$$

z_0 and v_R are defined as:

$$z_0=h-a \quad (56)$$

$$v_R=\frac{2\pi f}{k_R} \quad (57)$$

where f is the frequency.

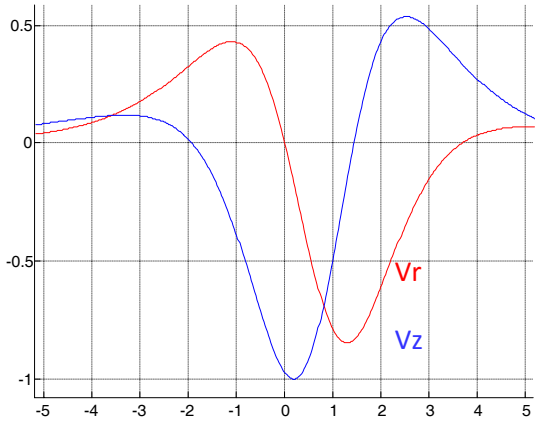

Figure 3: normalized Rayleigh wave particle velocity emitted from a buried crack located at 5 mm from the surface, propagating from 1mm to 5 mm at a velocity of 2000m/s, the observation point is located at (r=100mm,θ=0,z=0) .

We have compared these curves with the result of Harris and Pott [1] shown on Figure 4 obtained from an integral formulation in which they have combined Rayleigh wave Green function and the bulk waves emitted by the starting of the crack propagation. The bulk waves emitted by the crack were calculated by a ray method in the time domain. The displacement at the surface of the newly cracked material takes the functional form $F(t-\frac{r}{V_{tip}})$ where:

$$F(t-\frac{r}{V_{tip}}) = H(t)U\left(t-\frac{r}{V_{tip}}\right)^{1/2} \qquad (58)$$

r is the position of the crack tip, V_{tip} is the crack tip velocity, H is the Heaviside function and U is a constant that depends on the fracture process.

The integral was evaluated by separating the contribution of compressional and shear wave's parts and selecting their wave fronts to be the surface of integration. Then the stationary phase technique was applied to calculate the displacement in the frequency domain. The particle velocity of the emitted Rayleigh wave was approximated in the time domain near the Rayleigh arrival time.

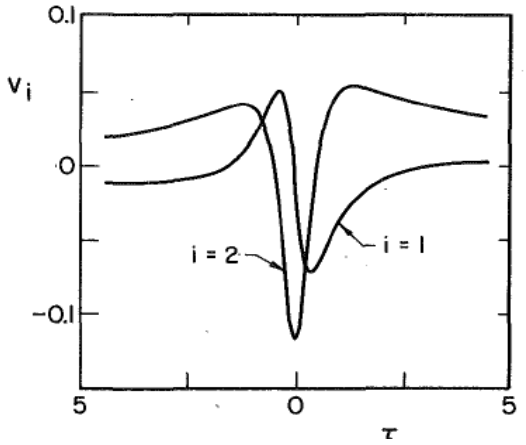

Figure 4: The normalized components of the Rayleigh-wave particle velocity at the surface, from the starting of the propagation of buried crack of radius a, plotted against $\tau = t\,{}^{v_R}\!/_{z_0} - {}^{x}\!/_{z_0}$ ($i=2$ correspond to the vertical velocity and $i=1$ corresponds to the velocity component along the x axis), $V_{tip} = 0.5\,{}^{\omega}\!/_{k_t}$, ${}^{x}\!/_{z_0} = 20$ and ${}^{z_0}\!/_{a} = 2$

Differences between Figure 3 and 4 can have several explanations. In fact, the result presented in figure 3 is obtained by the use of the crack opening displacement at all points of the crack and figure 4 present the velocity of the emitted wave from the starting of faulting event considering only the crack tip velocity. In addition, the time dependence of the displacement at the surface of the crack are different which is given by Eq. (53) and (58).

On the other hand, our integral formulation combines directly the COD and the Rayleigh wave Green functions. In the case of Harris and Pott model the integral formulation combines the bulk waves emitted from the crack approximated at the Rayleigh wave arrival time and Rayleigh wave Green functions.

We have simulated the Rayleigh wave particle velocity by considering the time dependence of the displacement at the surface of Eq. (58).

The COD can be written as:

$$\Delta u(t,\rho) = 2UF(t-\frac{\rho-\rho_0}{V}) + \Delta u(t_0) \qquad (59)$$

Where $\rho_0 = l_0/2$ is the initial radius of the crack and $\Delta u(t_0)$ is the crack opening displacement at $t=0$.

Figure 5 shows the Rayleigh wave particle velocity emitted the crack under stress.

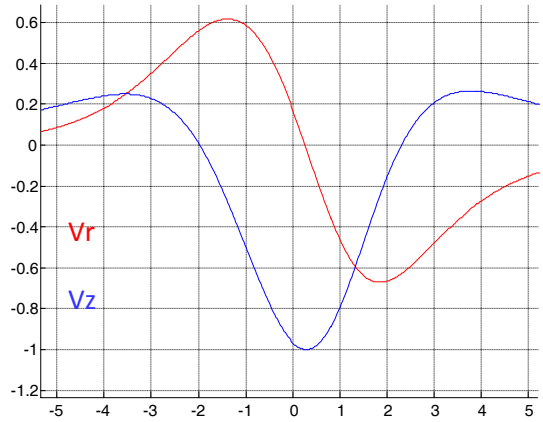

Figure 5: normalized Rayleigh wave particle velocity emitted from a buried crack located at 5 mm from the surface, propagating from 1mm to 5 mm at a velocity of 1600m/s, the observation point is located at (r=100mm,θ=0,z=0).

The result of figure 5 is closer to the result of Harris. The use of the same time dependence of the displacement at the surface of the crack gives a better agreement between both models.

4. Conclusion

We have developed an integral formulation to predict Rayleigh wave emitted from a crack under stress combining Rayleigh wave Green function and the crack opening displacement (COD) obtained from a fracture mechanic's model.

Comparison with literature showed a satisfying agreement even if the two models are different and not based on the same approximations and hypotheses

The use of the same time dependence of the AE source improves the agreement between both models.

References

1. G. P Harris, J Pott "Surface Motion Excited by Acoustic Emission from a Buried Crack", J. Appl. Mech. 51, 77-83 (1984)
2. J D Achenbach , A K Gautesen, H McMaken, *Ray methods for waves in Elastic solids*, Pitman publishing INC (1982)
3. J D Achenbach "Combination of a virtual wave and the reciprocity theorem to analyse surface wave generation on a transversely isotropic solid", Philosophical Magazine 85, 4143-4152 (2005)
4. J D Achenbach, Reciprocity in elastodynamics, Cambridge University Press (2003)